

FINITE ELEMENT MODEL OF HUMAN LOWER EXTREMITIES IN A FRONTAL IMPACT

Ellen Wykowski, Ruprecht Sinnhuber
Volkswagen AG, Wolfsburg, Germany

Hermann Appel
Institute of Road and Railway Traffic, Berlin Technical University, Germany

ABSTRACT

Over the past several years, the use of advanced safety belt and airbag systems in passenger cars had led to a reduction of severe head and chest injuries. Attention has therefore become more focused on lower limb injuries. These are not necessarily life threatening, but very often cause considerable pain and frequently require long-term treatment and rehabilitation and they can even result in permanent disability.

This paper presents an FE model of human lower extremities in PAM-CRASH™ - code as part of a collaborative effort between Volkswagen AG, Wolfsburg, Germany and Engineering Systems International (ESI), Rungis, France.

The model includes the ankle/foot complex (ESI) and the tibia, fibula, patella, and femur as well as some of the knee ligaments (VW) with the approximate anatomical structure and a mass distribution of a 50th percentile male. It replaces the lower extremities of a 50th percentile HIII dummy and is connected with the pelvis of the dummy.

This model will be used in an effort to investigate injury mechanisms during a frontal impact. The FE dummy with the FE human legs is placed in a car model which has a simplified interior structure. The objective of this paper is to analyse the loadings and kinematics of the legs for different combinations of intrusion depth and intrusion velocity (of the foot rest, the pedals, the steering wheel and the dashboard).

FREQUENCY AND SEVERITY OF LOWER LIMB INJURIES of belted vehicle occupants in traffic accidents are provided in a brief overview based on the VW accident database. The VW accident database contains information on traffic accidents collected by the Accident Research Unit of Medical University (MUH) Hanover on behalf of the Federal Highway Research Institute (BASt - Bundesanstalt für Straßenwesen). Information regarding approximately 8000 traffic accidents is currently stored in the VW database.

Figure 1 depicts the risk of injury to various parts of the body of belted occupants in passenger cars for all collision types. Injuries to the lower limbs occupy third place in terms of frequency with a share of 15.7%, preceded by head and chest injuries. A detailed investigation of leg and foot injuries during frontal collisions shows that bone injuries have the highest frequency (Fig. 2). Bone injury is defined to be open and closed

fractures as well as fractures with or without luxation or dislocation of vessels respectively.

Fig. 1 - Injury risk for different parts of the body for all collision types for belted front and rear occupants of passenger vehicles

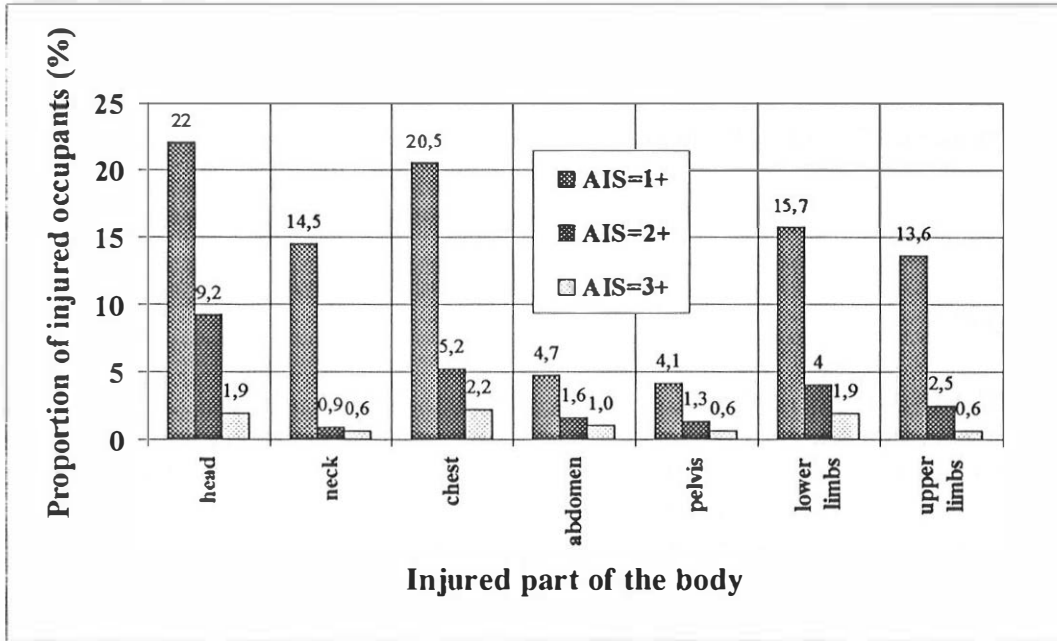


Fig. 2 - Number of leg injuries in frontal collision for belted front seat occupants

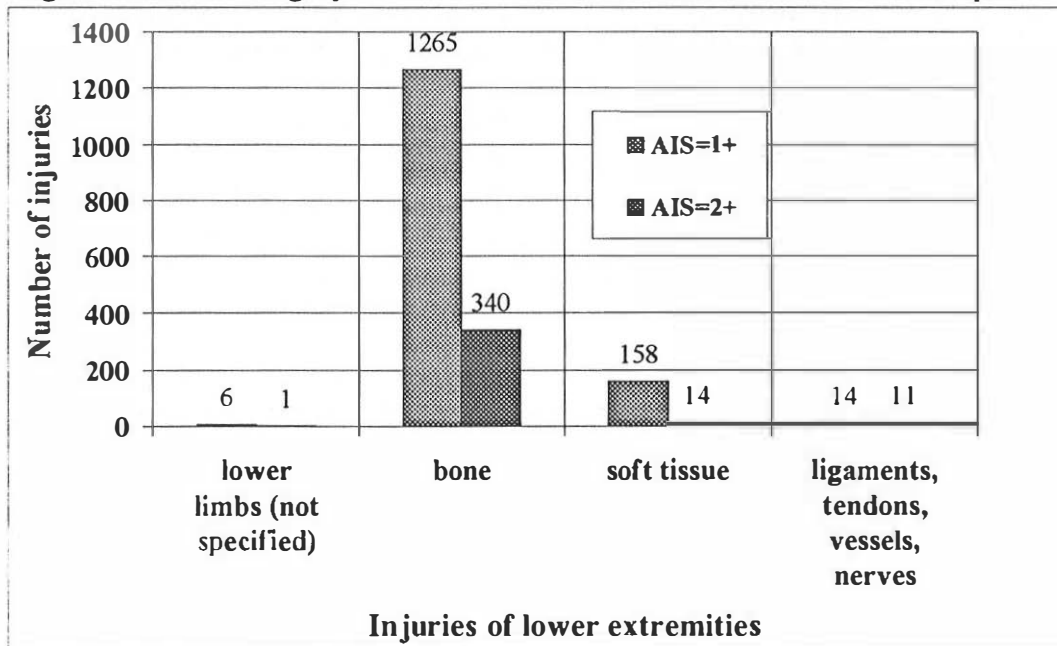


Figure 3 represents bone injuries AIS=2+ for the lower extremities for belted drivers only in frontal collisions. For drivers, those portions of the lower extremities that are at greatest risk are the patella, the femur shaft, ankle joint, the tibia, the fibula, ankle and the middle foot.

Investigation shows that bone injuries play an important role as far as lower extremities are concerned. For this reason, the main emphasis in the FE model of human legs is placed on the bones. Table 1 lists the injury sources for the leg injuries that are recorded in the database. Contact with the instrument panel and intruding surfaces are the primary source of injury followed by the pedals, the front partition and the foot room. The results obtained in this analysis are consistent to earlier investigations e.g. Thomas 1995, Huelke1991, Otte 1992, Morgan 1991 and others. The most important influencing factors for lower limb injuries are shown in Figure 4, but the most likely injury mechanism is the contact with the vehicle interior caused by the relative movement of the occupant.

Fig. 3 - Bone injuries AIS=2+ for lower extremities in frontal collision for belted drivers

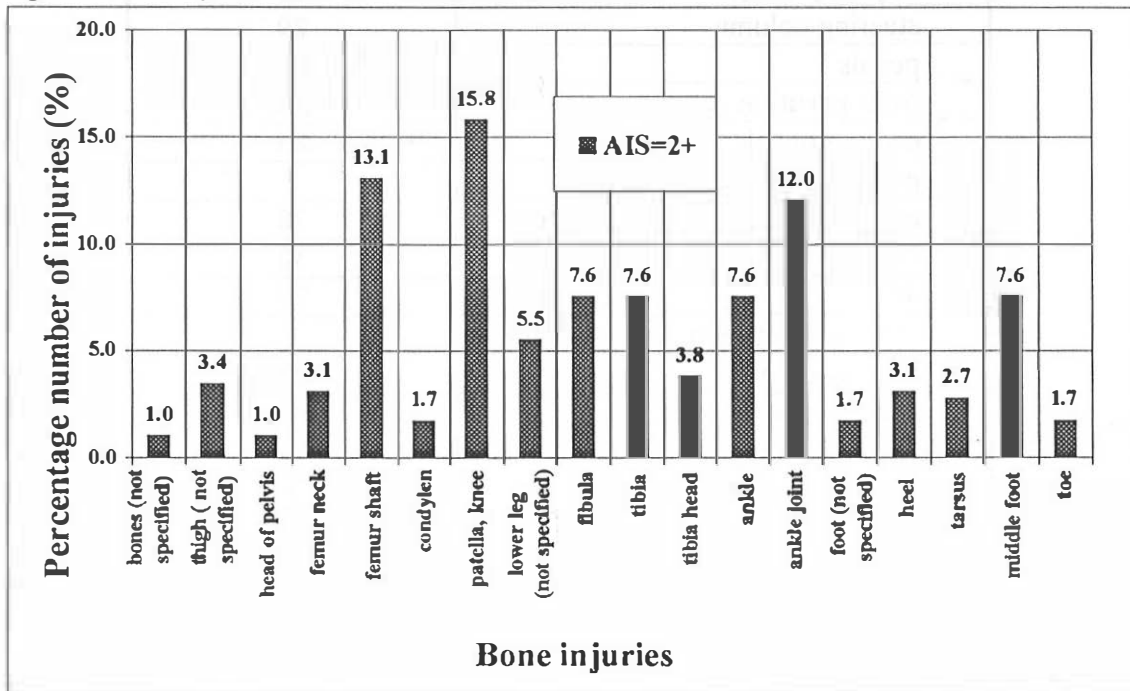


Fig. 4 - Principal factors influencing lower limb injuries

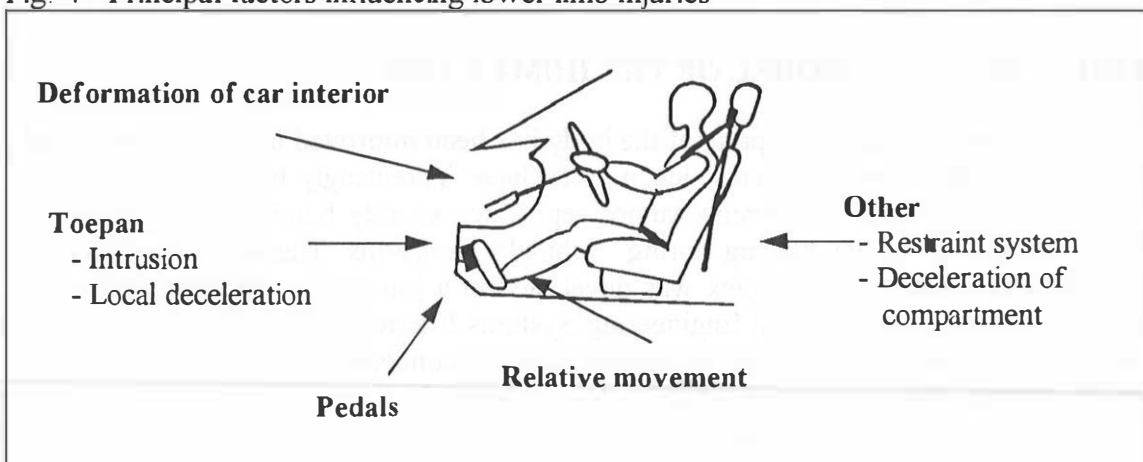


Table 1 - Sources of leg injuries AIS=1+ for all collision types

	Number of injuries
front passenger compartment	125
instrument panel	1085
radio	4
heater, ventilation	1
gear shift lever	12
ignition lock	6
steering wheel	38
foot space area	313
A-pillar, lower	25
steering column	29
pedals	234
front partition	116
centre console	85
parking brake	2
other foot space	38
interior	38
door	27
structure between A & B pillars	1
door structure	22
door panelling	81
door mounting	14
vehicle equipment	7
belt webbing	13
belt latch	2
seat squab	6
backrest	3
unknown	143

FINITE ELEMENT MODEL OF THE HUMAN LEG

As protection of the upper parts of the body has been improved by supplemental airbag and safety belt restraint systems, leg injuries have increasingly become the subject of many research efforts. A dummy cannot reproduce exactly human leg kinematics and loads caused by impact loading during vehicular collisions. Therefore a mathematical model of the human leg complex was developed in a joint effort between Volkswagen AG, Wolfsburg, Germany and Engineering Systems International (ESI), Rungis, France. This model seeks to reveal the injury mechanisms concerning leg injuries and thus to enable further improvements in vehicle safety to be made.

The ankle/foot complex was modelled and validated by ESI and has been documented in previous papers (Beaugonin 1995, 1996, 1997). The modelling and first validation of the knee complex (the femur, the tibia and the patella), the connection with the foot, and the connection of the legs with the dummy was undertaken by VW. The validation for

the complete model is based upon investigations carried out by the Institute of Forensic Medicine, University of Heidelberg, Germany (Schueler 1995, 1996).

Table 2 - Modelled FE Parts of human lower extremities

Bone	Ligament/Tendon/Retinaculum
Femur	Tendon calcaneus (Achilles)
Patella	Lig. anterior talo-fibular
Tibia	Lig. anterior tibio-fibular
Fibula	Lig. anterior tibio-talar
Talus	Lig. calcaneo-fibular
Calcaneus	Retinaculum flexor
Os naviculare	Retinaculum inferior extensor
Os cuboideum	Retinaculum inferior peroneal
Ossa cuneiformia	Lig. posterior tibio-fibular
Ossa metatarsalia	Lig. posterior talo-fibular
Phalangen	Lig. posterior tibio-talar
	Retinaculum superior peroneal
	Retinaculum superior extensor
	Lig. tibio-calcanean
	Lig. tibio-navicular
	Lig. collaterale laterale
	Lig. collaterale mediale
	Lig. patellae
	Lig. cruciatum posterius
	Lig. cruciatum anterius
	Lig. meniscofemorale posterius
	Lig. capitis fibulae anterius
	Meniscus

The model consists of bones, ligaments, tendons, and some muscles with the approximate anatomical structure and a mass distribution of a 50th percentile male. The data for geometry were digitised by Viewpoint Datalabs. A complete list of all human parts involved is provided in Table 2. The bone was modelled as a rigid body with the compact bone as shell elements and the spongy bone as solid elements. The soft tissue - ankle/knee ligaments, retinacula and Achilles tendon - are modelled by membranes, and the foot ligaments by bar elements. The material properties were selected from Yamada 1970 for compact bone and some ligaments, spongy bone from Carter 1977. The connection between two bones was modelled with the joints listed in Table 3.

Table 3 -Joint description

Joint description:	Tibiotarsal joint
	Subtalar joint
	Mediotarsal joint
	Tarsometatarsal joint
	Cuneionavicular joint
	Metatarsophalangeal joint
	Knee joint

The material properties which have been used for the simulation are listed in Table 4 and 5.

Table 4 - Material properties of bones (Yamada 1970, Carter 1977)

	Young's modulus (N/mm ²)	Poisson ratio
Compact bone		
Calcaneus	15000	0,29
Os cuboideum	15000	0,29
Ossa cuneiforma	15000	0,29
Ossa metatarsalia	1000	0,29
Os naviculare	15000	0,29
Phalangen	1000	0,29
Talus	15000	0,29
Femur	17600	0,326
Tibia	18400	0,326
Fibula	18900	0,326
Patella	1760	0,326
Spongy bone		
Calcaneus	531	0,3
Os cuboideum		
Os naviculare		
Talus		
Femur		
Tibia		
Fibula		
Patella		

Table 5 - Material properties of knee ligaments Density = 1e-06 kg/mm³
(layered material for membrane elements)

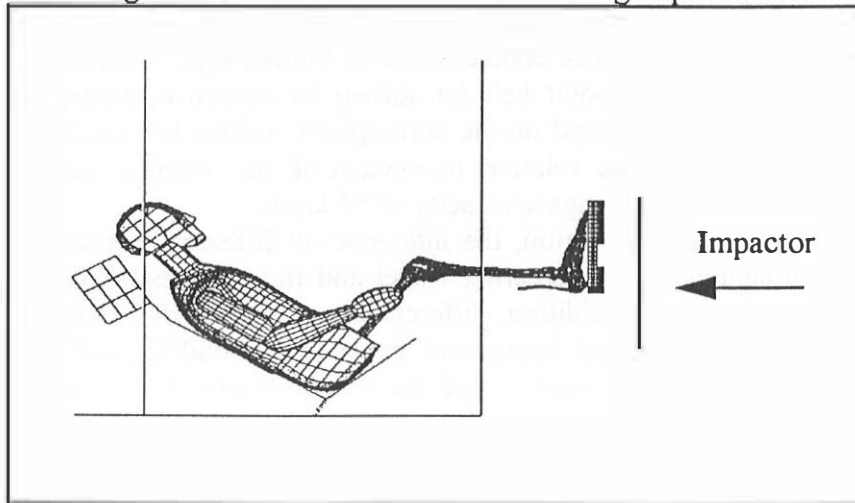
	Fiber layer 1		Fiber layer 2	
	Young's modulus (N/mm ²)	Shear modulus (N/mm ²)	Young's modulus (N/mm ²)	Shear modulus (N/mm ²)
Lig. collaterale laterale	190	73	170	65
Lig. collaterale mediale	80	30	70	27
Lig. patellae	400	158,8	360	138,5
Lig. cruciatum posterius	30	11,5	27	10,4
Lig. cruciatum anterius	60	23	55	21
Lig. meniscofemorale posterius	40	15,4	37	14,2

This paper contains only a brief description of the validation of the model, particularly the knee complex. A full description of the validation of the model is beyond the scope of this paper and will be documented in (Wykowski).

The model was validated using tests performed by the Institute of Forensic Medicine, University of Heidelberg, Germany (Schueler 1995, 1996). The Post Mortem Human Subjects (PMHS) tests were utilized for the classification of injury mechanism and

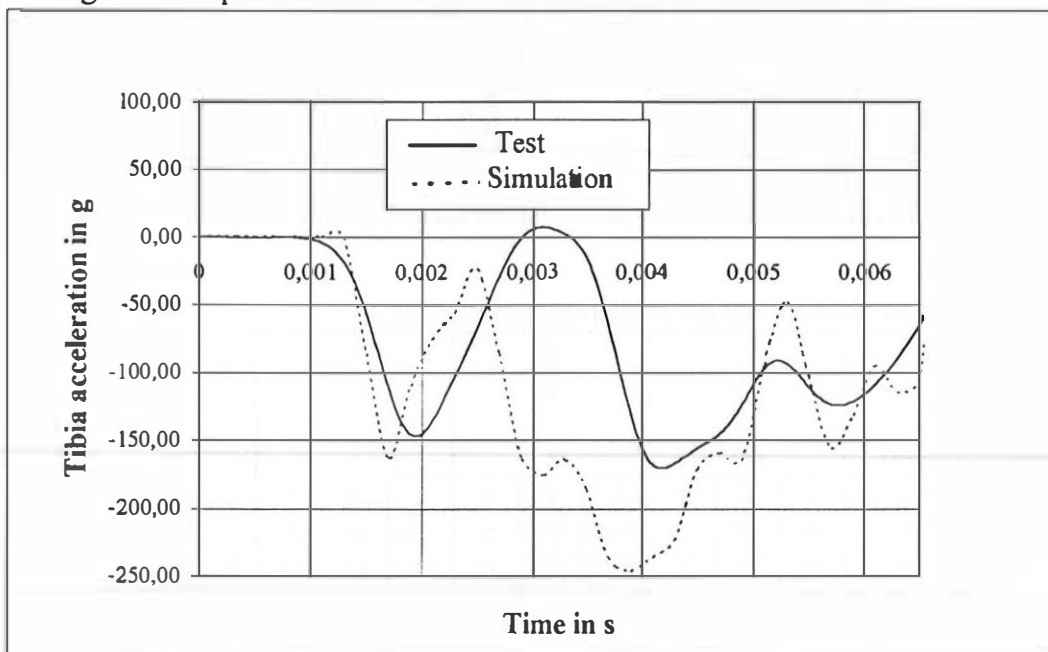
tolerance limits of the lower legs. Uninjured PMHS were impacted at the plantar foot surface by a coaxial impactor. The model of the PMHS leg impactor test is shown in Figure 5.

Fig. 5 - Model to simulate the PMHS leg impactor test



The acceleration of the tibia was recorded during the experiments. The accelerometer was mounted at the distal part of the tibia. The impact forces as well as acceleration of the foot was measured with transducers located in a special shoe designed for this purpose. In Figure 6 a comparison of acceleration of the tibia for the PMHS and the results of computer simulation is shown. Good agreement can be seen at the beginning of the curves. The end of the curves are different because of different behaviour of the impactor after the initial impact. The tests were documented by a high speed camera to permit comparison of the kinematics of the entire leg.

Fig. 6 - Comparison of acceleration of the tibia between test and simulation



FRONTAL IMPACT WITH FE HUMAN LEGS AND FE DUMMY IN A SIMPLIFIED INTERIOR VEHICLE STRUCTURE

The FE model of human lower limbs developed is used in order to investigate leg loads and kinematics during a frontal offset crash. Therefore, the FE dummy with FE human legs is placed in a car model with a simplified interior structure (Figure 7). The interior compartment contains a steering wheel, an instrument panel, pedals, a foot rest and a floorboard which describe possible contact areas of human legs. The dummy is placed in a seat and restrained by a 3-point belt (an airbag to reduce occupant loading is not modelled). The right foot is placed on the brake pedal and the left on the foot rest. The simulation time is 150 ms. The relative movement of the dummy corresponds to an 40 % offset frontal crash at an impact velocity of 56 km/h.

By means of computer simulation, the influence of different intrusion depths of the pedals, the instrument panel, the steering wheel and the foot rest at different intrusion velocities are investigated. In addition, different contacts with different force/deflection characteristics between legs and instrument panel (hard, middle, soft) are examined. Table 6 depicts the simulation matrix used for two different contact stiffnesses of the dashboard.

In addition, measuring points were placed in the human tibia so that the axial compression forces (Force_z), the bending moments in lateromedial (Moment_x) and anteroposterior direction (Moment_y) can be calculated.

Fig. 7 - FE dummy and FE human leg placement in the vehicle

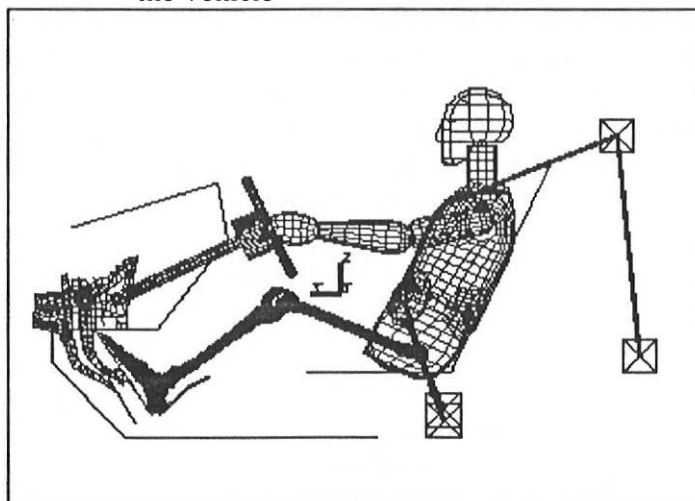


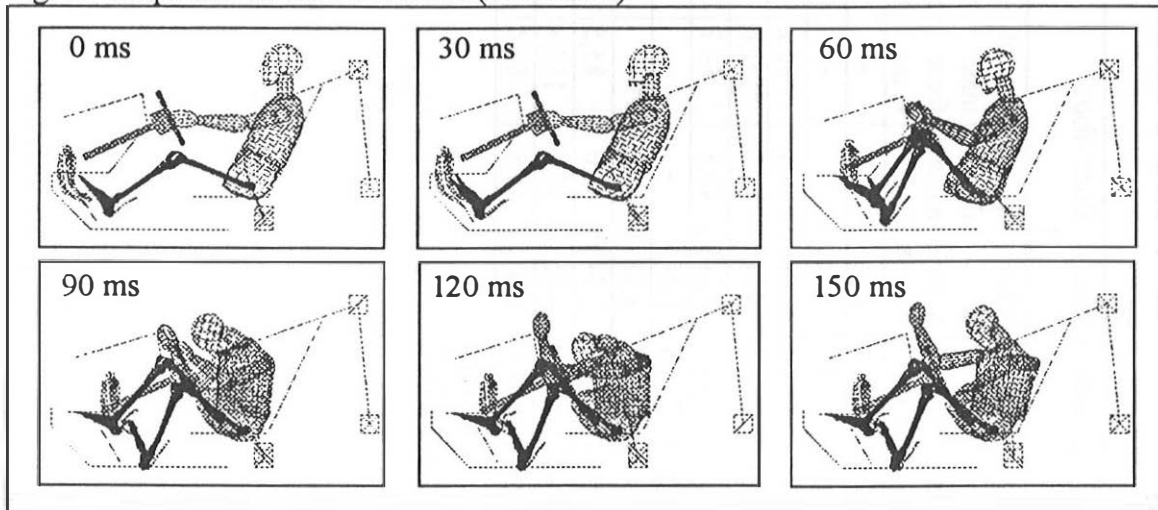
Table 6 - Simulation matrix (maximum displacement in mm)

Test- NR.	1	2			3			4			5		
Velocity $v = f(s, t)$	$v=0$	$v/2$			v			$v/2$			$2v$		
Displacement	$s=0$	$s/2$			s			s			s		
Direction	x y z	x	y	z	x	y	z	x	y	z	x	y	z
Pedals	0	120	40	25	240	80	50	240	80	50	240	80	50
Foot rest	0	65	22	7	130	45	15	130	45	15	130	45	15
Dashboard	0	40	0	10	80	0	20	80	0	20	80	0	20
Steering wheel	0	50	50	50	100	100	100	100	100	100	100	100	100

RESULTS

Because of the limited biomechanical data existing today, this paper can only analyse trends regarding the influence of vehicle components on occupant kinematics and leg loads kinematics utilising FE legs developed. All results have been filtered with the SAE 60-5 filter. A time sequence of the FE simulation is shown in Fig. 8. The movement of the dummy between 0 - 150 ms for the force limited contact of 8 kN and maximum displacement (Test no. 3) is shown.

Fig. 8 - Sequence of FE simulation (Test no. 3)



In this sequence, the right leg has contacted the steering wheel and is entrapped between steering wheel and floor. The left leg has contacted the instrument panel and is entrapped between foot rest and lower portion of the dashboard.

The various contacts for the right and left leg are listed in Tables 7 and 8. The right leg contacted the steering wheel. The right foot contacted the floor and the lower dashboard. All forces were related to the contact forces of the right foot of Test no. 1 without intrusion ($s=0$, $v=0$). The highest loadings are found in Test no. 5.

Within the investigation, the left leg contacted the steering wheel and the lower dashboard. The two dashboard contact loads (8 and 11 kN) selected have only a minor influence on leg loads.

For the purposes of this discussion of the influence of the intrusion and intrusion velocity of leg loads, all loads are related to the sled simulation No.1 without intrusion. An evaluation of the relative axial compression force and relative bending moments in the tibia (Figures 9, 11 and 13) shows that with the same intrusion depth but with different velocities, the axial compression forces and bending moments are higher at higher velocities. Intrusion velocity, not intrusion depth is the dominant parameter for leg loads.

Figures 10, 12 and 14 show the relative axial compression force and relative bending moments / time history for the right leg with the same intrusion velocity but with different intrusion depths ($s/2$, s) in comparison to the axial compression force and bending moments / time history for $s=0$ and $v=0$. At the beginning, the values are nearly identical. After 65 ms, bending moments in the tibia increase with the higher dorsiflexion caused at the greater intrusion depth.

The other measuring points on the left and right leg show the same tendency.

Right leg																	
contact definition	brake/foot			dashboard front / tibia		steering wheel/ patella/tibia			steering wheel/femur			floor /foot			lower dashboard/foot		
	time of first contact in ms	time of max. force in ms	value of relative force *			time of first contact in ms	time of max. force in ms	value of relative force *	time of first contact in ms	time of max. force in ms	value of relative force *	time of first contact in ms	time of max. force in ms	value of relative force *	time of first contact in ms	time of max. force in ms	value of relative force *
1 11 kN	8,6	30,0	1	-	-	134,6	140,4	0,15	135,6	140,8	1,08	-	-	-	30,4	33,9	0,02
2 11 kN	8,6	36,2	1,96	-	-	50,8	80,6	2,60	49,4	71,0	3,56	-	-	-	29,0	67,0	0,34
3 11 kN	8,6	36,0	3,16	-	-	44,5	110,0	2,71	45,0	51,6	4,90	64,4	82,2	1,08	29,0	36,6	0,23
4 11 kN	8,6	68,4	2,04	-	-	50,6	72,0	1,79	49,4	71,6	3,75	95,0	131,0	0,60	28,6	67,6	0,42
5 11 kN	8,6	36,0	4,92	-	-	40,2	47,4	0,85	40,8	47,6	8,24	45,3	64,3	1,81	28,6	36,6	0,84
1 8 kN	8,6	30,0	1	-	-	134,6	140,6	0,15	135,6	140,8	1,10	-	-	-	28,8	33,0	0,43
2 8 kN	8,6	67,6	1,98	-	-	50,8	80,6	2,54	49,4	70,8	3,48	-	-	-	29,4	67,4	0,33
3 8 kN	8,6	36,0	3,14	-	-	44,6	70,6	2,6	45,2	70,0	5,34	65,0	85,5	0,93	28,8	36,4	0,28
4 8 kN	8,6	68,8	2,17	-	-	50,6	100,8	2,87	49,4	101,0	4,65	95,6	117,8	0,44	29,0	63,6	0,55
5 8 kN	8,6	36,0	4,92	-	-	40,1	48,6	0,96	40,8	47,6	8,61	44,8	69,4	2,15	29,0	37,0	0,79

Table 7 - General view of contact definitions - initial and maximum forces- for the right leg

Two different force limited contacts 11 kN and 8 kN for dashboard were defined.

* related to the foot/brake contact force at s=0

Left leg																		
contact definition	foot rest/foot			dashboard front/tibia			steering wheel/ patella/tibia			steering wheel/femur			floor/foot			lower dashboard/foot		
	time of first contact in ms	time of max. force in ms	value of relative force *	time of first contact in ms	time of max. force in ms	value of relative force *	time of first contact in ms	time of max. force in ms	value of relative force	time of first contact in ms	time of max. force in ms	value of relative force *	time of first contact in ms	time of max. force in ms	value of relative force *	time of first contact in ms	time of max. force in ms	value of relative force *
1 11 kN	27,6	37,7	1	-	-	-	-	-	-	-	-	-	-	-	56,8	62,3	0,17	
2 11 kN	27,6	36,8	1,75	-	-	-	-	-	84,6	89,2	0,58	-	-	-	60,6	70,6	0,08	
3 11 kN	27,6	36,6	2,16	63,0	87,8	0,01	51,4	56,3	51,0	84,5	0,91	-	-	-	62,4	94,6	0,14	
4 11 kN	27,6	36,8	1,72	-	-	-	-	-	83,0	89,8	0,68	-	-	-	59,4	65,4	0,17	
5 11 kN	27,6	36,4	2,08	73,4	83,4	0,001	-	-	64,0	103,0	0,95	-	-	-	65,4	75,6	0,22	
1 8 kN	27,6	37,6	1	-	-	-	-	-	-	-	-	-	-	-	57,0	63,4	0,22	
2 8 kN	27,6	36,8	1,75	115,5	133,4	0,0001	112,5	124,4	84,6	89,2	0,60	-	-	-	60,4	70,8	0,10	
3 8 kN	27,6	36,6	2,16	63,0	85,3	0,0056	51,4	56,3	51,0	94,5	0,88	-	-	-	62,4	121,0	0,10	
4 8 kN	27,6	36,8	1,72	-	-	-	-	-	82,4	126,8	0,54	-	-	-	59,4	65,6	0,17	
5 8 kN	27,6	36,4	2,08	-	-	-	-	-	68,0	119,0	1,32	-	-	-	-	-	-	

Table 8 - General view of contact definitions - initial and maximum forces- for the left leg

Two different force limited contacts 11 kN and 8 kN for dashboard were defined.

* related to the foot/foot rest contact force at s=0

Fig. 9 - Relative axial compression forces of the tibia for the right lower leg

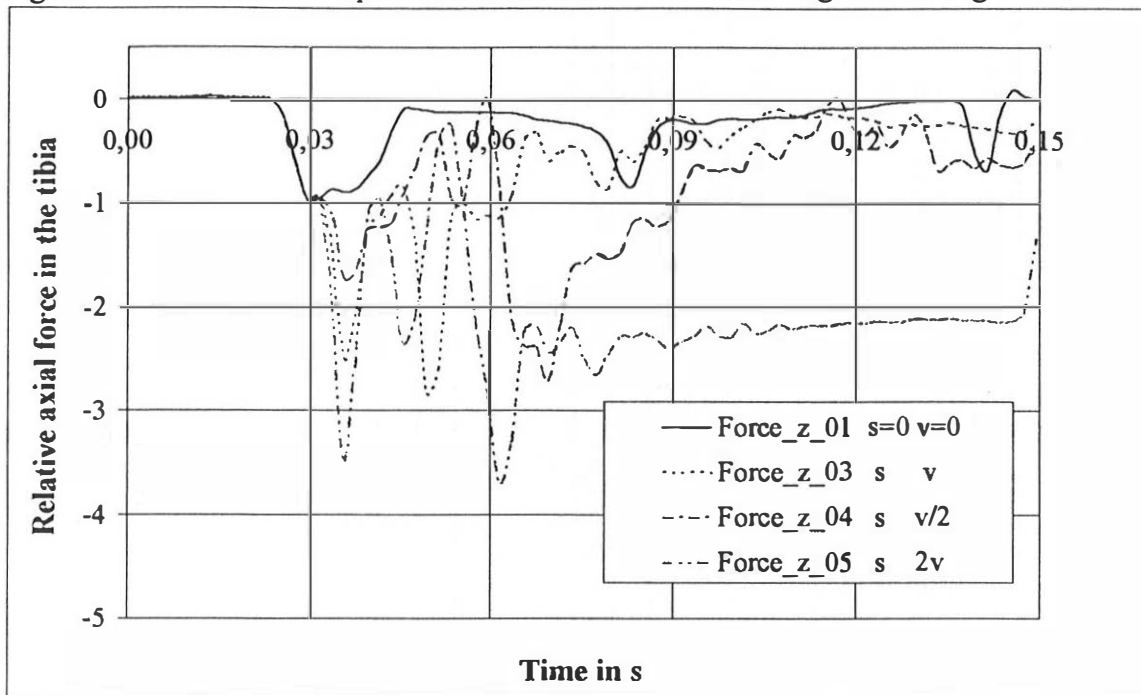


Fig. 10 - Relative axial compression forces of the tibia for the right lower leg

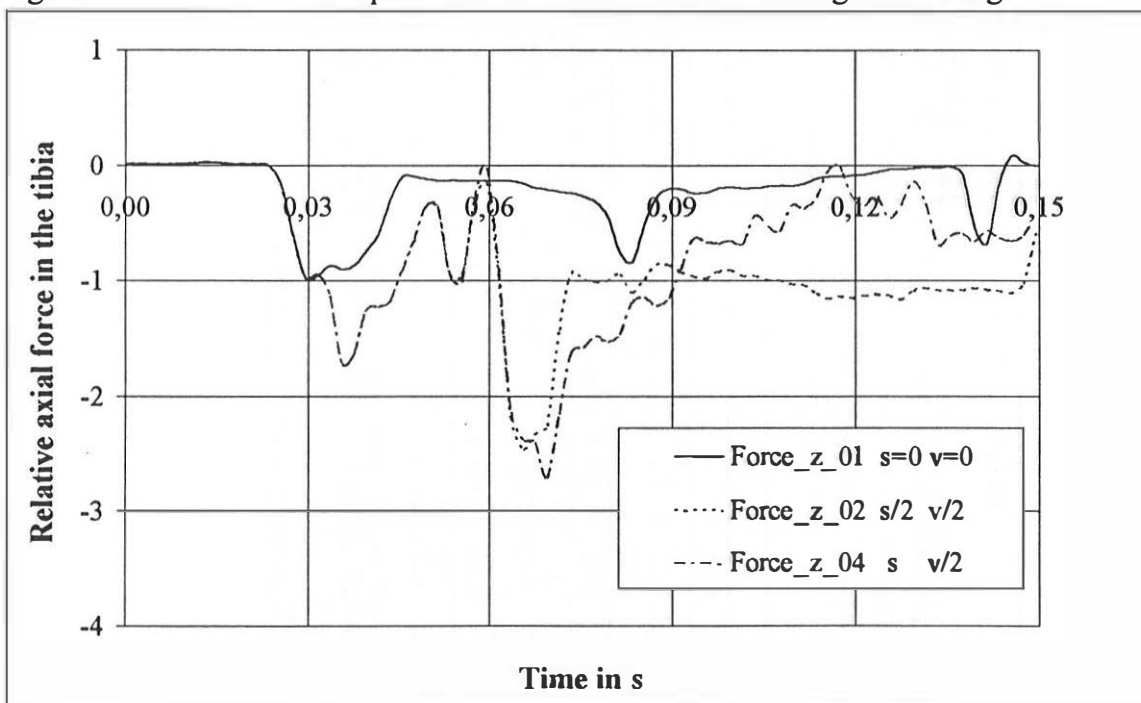


Fig. 11 - Relative bending moment in lateromedial direction of the tibia for the right lower leg

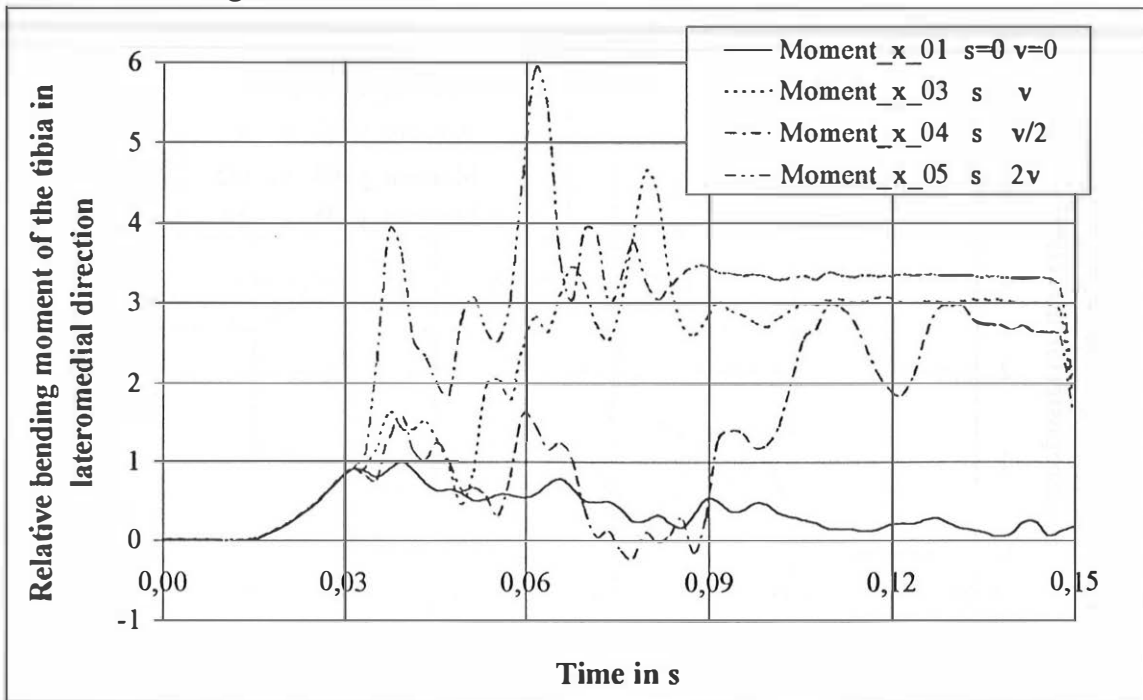


Fig. 12 - Relative bending moment in lateromedial direction of the tibia for the right lower leg

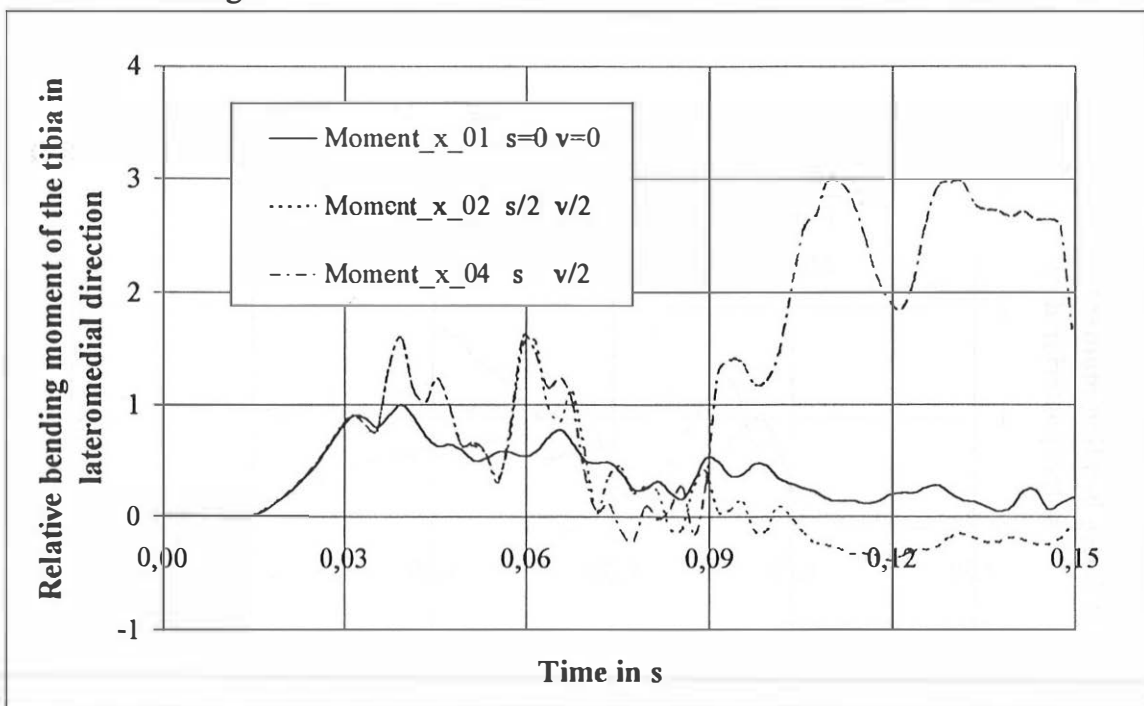


Fig. 13 - Relative bending moment in anteroposterior direction of the tibia for the right lower leg

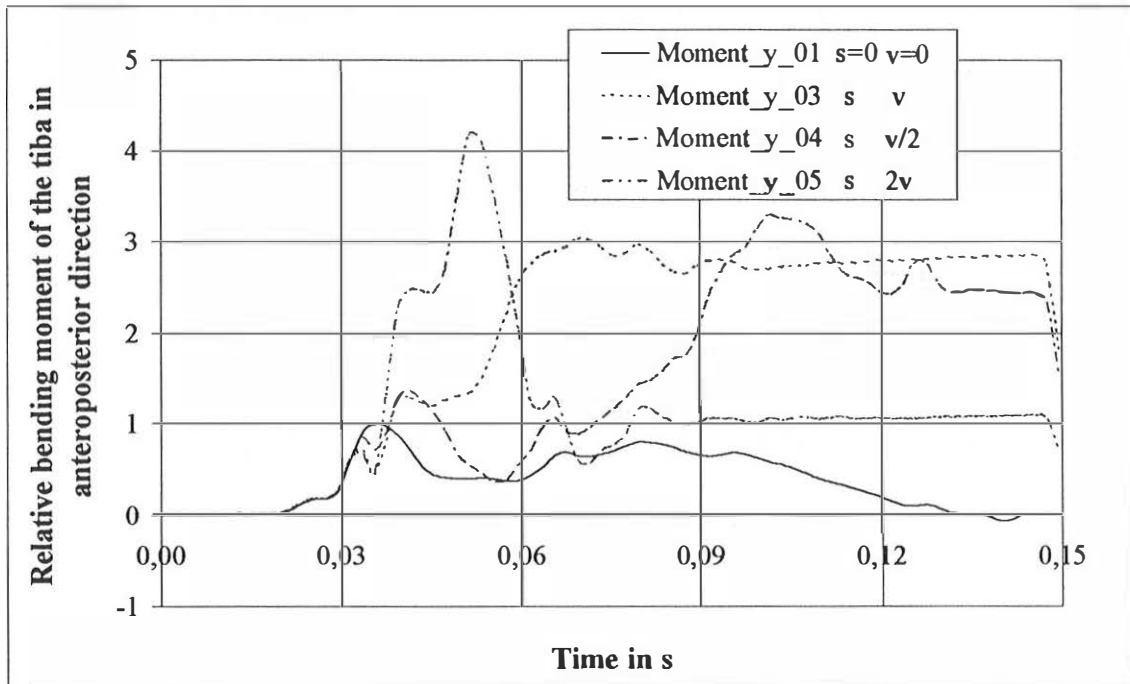
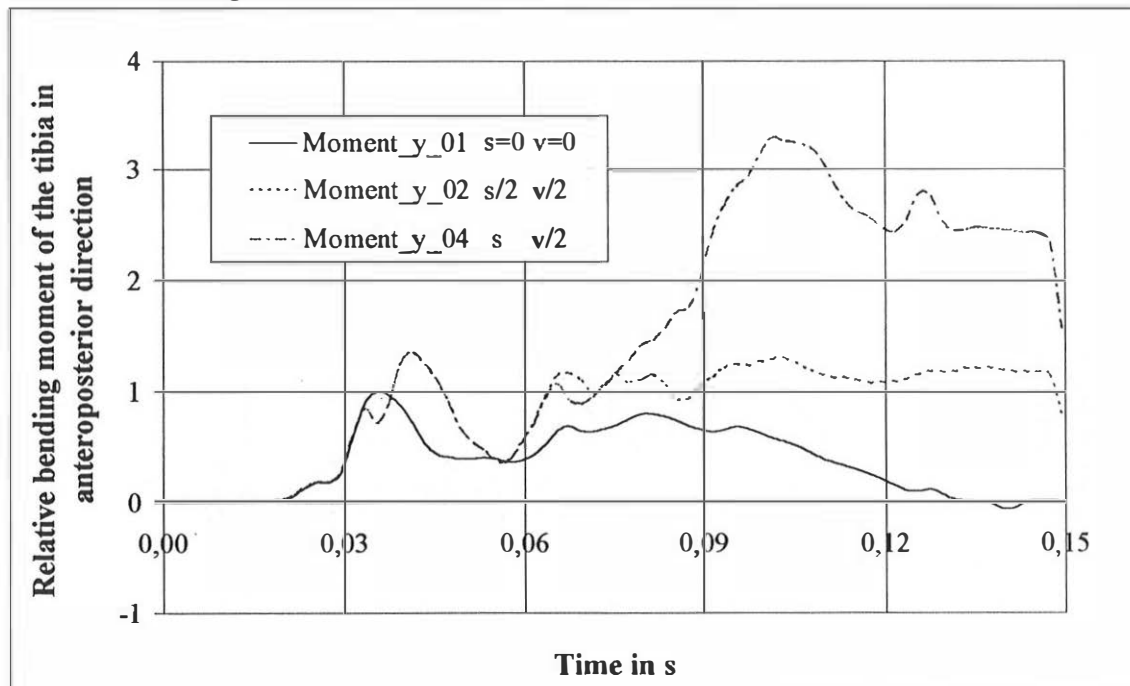


Fig. 14 - Relative bending moment in anteroposterior direction of the tibia for the right lower leg



DISCUSSION

First qualitative analysis of leg loadings with FE human legs were performed. Up to a certain limit, intrusion velocity and not intrusion depth is the main parameter for bending moments and forces applied to the bones. The lowest leg loadings were found in Test no. 1 with no intrusion and no intrusion velocity. The highest leg loadings were found in Test no. 5 with maximum intrusion and double intrusion velocity.

Because of the limited biomechanical data available today, validation of the relative forces associated with the FE leg model and bending moments could only be calculated. The intention was to demonstrate qualitative influence of different intrusion depths and velocities of the dashboard, steering wheel, pedals, and foot rest on the leg loadings. It must still be investigated how the calculated loadings and kinematics correlate with the real crash behaviour of human beings.

To investigate the absolute influence of the parameters listed on leg loads and kinematics, further biomechanical knowledge is required for the validation of the FE leg model. In order to analyse injury mechanisms during frontal impacts, a deformable FE leg model must be used.

CONCLUSIONS

Based upon biomechanical data, an FE model of human legs has been developed with rigid bodies. The model provides contact forces as well as forces and moments in the joints. With this FE model, an initial parametric analysis has been made which revealed the following:

Up to a certain limit intrusion velocity not intrusion depth is the main parameter for leg loads in frontal collisions.

For the final validation of the FE legs developed, further biomechanical research is necessary to be able to predict the loadings and kinematics of human lower limbs during real accidents.

The investigations in this paper are the beginning of a more detailed analysis of injury mechanisms of the lower limbs. Other foot positions (plantarflexion, dorsiflexion, eversion and inversion) will also be analysed. With the use of deformable FE bones, the stress sequences during the impact can be analysed in the future.

It will also be possible to model people of different ages and/or size by changing material properties or scaling the elements. The FE model of the leg presented in this paper is the first step in the investigation of the influence of vehicle-related measures on the leg loads and kinematics. With the final validated model a tool will be available that will make it possible to develop further improvements especially for the human leg instead of the dummy leg. In this manner, human models will be utilised for FE simulations.

REFERENCES

- Carter, D.R.; Hayes, W.C. (1977): The Behaviour of Bone As Two-Phase Porous Structure, *Journal of Bone Joint Surgery*, V, 59A, pp 954-962
- Beaugonin, M.; Haug, E.; et al. (1995): A Preliminary Numerical Model of the Human Ankle Under Impact Loading, PLEI Conference, Washington, D.C., USA
- Beaugonin, M.; Haug, E.; Cesari, D.(1996): A Numerical Model of the Human Ankle/Foot Under Impact Loading in Inversion and Eversion, 40th Stapp Car Crash Conference, Society of Automotive Engineers
- Beaugonin, M.; Haug, E.; Cesari, D.; et al. (1996): The Influence of Some Critical Parameters on the Simulation of the Dynamic Human Ankle Dorsiflexion Response, 15th ESV Conference, Melbourne, Australia
- Beaugonin, M.; Haug, E.; Cesari, D (1997): Improvement of Numerical Ankle/Foot Model. Modelling of Deformable Bone, 41th Stapp Car Crash Conference, Society of Automotive Engineers
- Huelke, D.F.; Compton, T.W., et al. (1991): Lower Extremity Injuries in Frontal Crashes: Injuries, Locations, AIS and Contacts, 35th Stapp Car Crash Conference Proceedings, Society of Automotive Engineers
- Morgan, R.M.; Eppinger, R.H.; et al. (1991): Ankle Joint Injury Mechanisms for Adults in Frontal Automotive Impact, 35th Stapp Car Crash Conference Proceedings, Society of Automotive Engineers
- Otte, D. ; H.v. Rheinhaben, et al. (1992): Biomechanics of Injuries to the Foot and Ankle Joint of Drivers and Improvements for an Optimal Car Floor Development, 36th Stapp Car Crash Conference, Society of Automotive Engineers
- Schueler, F.; Mattern, R., et al. (1995): Injuries of the Lower Legs- Foot, Ankle Joint, Tibia; Mechanisms, Tolerance Limits, Injury-Criteria Evaluation of a Recent Biomechanic Experiment-Series, 1995 International IRCOBI Conference on the Biomechanics of Impact, Brunnen (Switzerland)
- Schueler, F.; Mattern, R., et al. (1996): Zur Verletzungsmechanik und Belastbarkeit der unteren Extremität, insbesondere des Fußes, Forschungsvereinigung Automobiltechnik e.V., FAT Schriftenreihe Nr. 130
- Thomas, P.; Charles, J. et al. (1995): Lower Limb Injuries- the Effects of Intrusion, Crash Severity and Pedals on Injury Risk and Injury Types in Frontal Collision, Stapp Car Crash Conference, Society of Automotive Engineers
- Yamada, H.; Editor Evans, F.G: (1970): *Strength of Biological Materials*, Williams & Wilkins Company, Baltimore
- Wykowski, E.: Entschärfung des Fußraumes zur Reduzierung der Beinverletzungen mit Hilfe von FE-Simulationen, Thesis, Berlin Technical University in preparation